Photodynamic therapy with an endocytically located photosensitizer cause a rapid activation of the mitogen-activated protein kinases extracellular signal-regulated kinase, p38, and c-Jun NH_2 terminal kinase with opposing effects on cell survival

Anette Weyergang, Olav Kaalhus, and Kristian Berg

Department of Radiation Biology, Institute for Cancer Research, The Norwegian Radium Hospital, Oslo, Norway

Abstract

Photochemical internalization (PCI) is a method for release of endosomally/lysosomally trapped drugs into the cell cytosol. PCI is based on photosensitizers that accumulate in the membranes of endosomes and lysosomes. Light exposure generates reactive oxygen species that cause membrane rupture and subsequently drug release. PCI can be considered as a combination therapy of photodynamic therapy (PDT) and the administrated drug. The present work reports on mitogen-activated protein kinase signaling after PDT with the endocytically located photosensitizer $TPPS_{2a}$ (*meso*-tetraphenylporphine with two sulfonate groups on adjacent phenyl rings) as used for PCI in two cancer cell lines: NuTu-19 and WiDr. Both extracellular signal-regulated kinase (ERK) and p38 were activated immediately after PDT. The photochemically induced ERK phosphorylation was enhanced by epidermal growth factor stimulation to a level above that obtainable with epidermal growth factor alone. Expression of the ERK phosphatase, MAPK phosphatase-1, was increased 2 h after PDT but was not the cause of ERK dephosphorylation observed simultaneously. A transient activation of c-Jun NH_2 terminal kinase was also observed after PDT but only in the NuTu-19 cells. Using suitable inhibitors, it is shown here that the p38 signal is a death signal, whereas c-Jun NH_2 terminal kinase rescues cells after PDT. No direct connection was observed between PDT-induced ERK activation and toxicity of the treatment. The present results document the importance of the mitogen-activated protein kinases in $TPPS_{2a}$-PDT-induced cytotoxicity. [Mol Cancer Ther 2008;7(6):1740–50]

Received 1/8/08; revised 3/6/08; accepted 3/10/08.

The costs of publication of this article were defrayed in part by the payment of page charges. This article must therefore be hereby marked *advertisement* in accordance with 18 U.S.C. Section 1734 solely to indicate this fact.

Requests for reprints: Anette Weyergang, Department of Radiation Biology, Institute for Cancer Research, The Norwegian Radium Hospital, Montebello, N-0310 Oslo, Norway. Phone: 47-22-93-46-36; Fax: 47-22-93-42-70. E-mail: anette.weyergang@rr-research.no

doi:10.1158/1535-7163.MCT-08-0020

Introduction

Photochemical internalization (PCI) is a novel technology for the release of endocytosed macromolecules into the cytosol (1, 2). The technology is based on the light activation of photosensitizers located in endocytic vesicles and the subsequent formation of singlet oxygen ($^1O_2$) and other reactive oxygen species. In this way, endocytosed molecules can be released from the endocytic compartments and reach their target of action before they are degraded in lysosomes (Fig. 1). PCI has been shown to stimulate intracellular delivery of a large variety of drugs that do not readily penetrate the plasma membrane, including type I ribosome inactivation proteins, ribosome inactivation protein–based immunotoxins, and DNA delivered as gene-encoding plasmids, or by means of adenoviruses or adenoassociated viruses, peptide nucleic acids, small interfering RNA, and chemotherapeutic agents such as bleomycin (3, 4). The PCI principle has also been documented in several animal models *in vivo* (5–8). In general, PCI can induce efficient light-directed delivery of macromolecules into the cytosol and may have a variety of useful applications for site-specific drug delivery, for example, in gene therapy, vaccination, and cancer treatment.

The optimal utilization of the PCI technology for cancer therapy is by photochemical delivery of targeted macromolecules, thereby exerting a three-way specificity of the treatment by the preferential retention of the photosensitizers in the neoplastic lesions, by light-directed activation of the therapeutic macromolecule, and by the linking of a targeting moiety to the therapeutic macromolecule. Epidermal growth factor (EGF) receptor (EGFR) is a widely used receptor for targeted delivery of anticancer therapeutics due to its overexpression in a large variety of tumors. PCI of EGFR-directed proteins toxins has been shown very promising both by using EGF and the monoclonal antibody cetuximab as targeting ligands (9, 10). PCI can be considered as a multimodality therapy of photodynamic therapy (PDT; treatment with photosensitizers and light) and treatment with the macromolecule of interest (Fig. 1). The

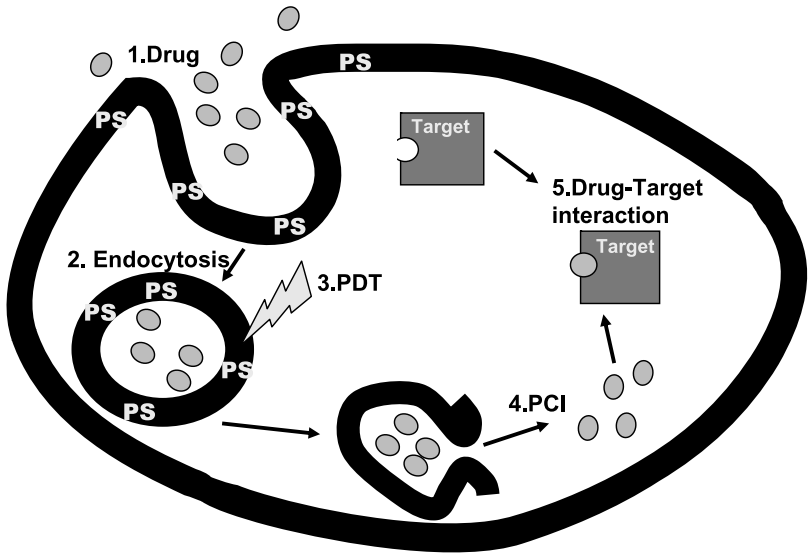

Figure 1. Illustration of the PCI principle. The drug (*1*) is taken into the cell by endocytosis (*2*) and is transported to an endocytic vesicle with photosensitizers localized mainly in its membrane. Light exposure of the photosensitizers (*3*) causes disruption of the membrane, and the drug escapes from the vesicle into the cytosol (*4*) were it interacts with its target (*5*).

mechanisms of PDT-induced cell death and the interplay with EGFR-targeted ligands, which have their own cellular and therapeutic effects, is therefore of interest in PCI of EGFR targeting drugs.

The mitogen-activated protein kinase (MAPK) pathway plays a critical role in cell proliferation, survival, angiogenesis, and metastasis. The MAPK family consists of the three kinases: the extracellular signal-regulated kinase (ERK), the stress-activated protein kinase/c-Jun NH_2 terminal kinase (JNK), and p38. The activity and the role of the MAPKs have, to some extent, been studied after PDT and are suspected to be of importance in the cellular processes controlling death and survival after oxidative stress (11–13). The activation patterns and functions of the MAPK after photochemical treatment are, however, strongly dependent of the cell type, photosensitizer, its cellular localization, and the light dose used. Little is known about the influence of photochemically activated and endocytically located amphiphilic photosensitizers as those used in PCI [e.g., *meso*-tetraphenylporphine with two sulfonate groups on adjacent phenyl rings ($TPPS_{2a}$)] on MAPKs and the role of MAPK activity for the outcome of this kind of PDT. We recently reported on photochemical effects on EGFR using $TPPS_{2a}$ as a photosensitizer and showed that the PDT regimen as used in PCI, inactivated EGFR in a dose-dependent manner in NuTu-19 cells but not in WiDr cells. The present report addresses the role of the three MAPKs: ERK, JNK, and p38 in $TPPS_{2a}$-mediated PDT. All the MAPKs, except JNK in WiDr cells, were activated shortly after PDT in both NuTu-19 and WiDr cell lines. Blocking the activation of the MAPKs after PDT and PCI with suitable inhibitors showed that the p38 activation serves as a death signal, the JNK activation serves as a rescue signal, and the ERK activation has no influence on the treatment outcome. The present results document the importance of MAPKs in the sensitivity to PDT and PCI.

Materials and Methods

Cell Culture and Cultivation

Two cell lines were used in this study: NuTu-19 rat epithelial ovarian cancer cell line (a gift from Dr. A.L. Major, University of Geneva) and WiDr human colorectal adenocarcinoma (American Type Culture Collection). Both cell lines were subcultured two to three times per week in RPMI 1640 (Sigma) supplemented with 10% FCS (Life Technologies), 100 units/mL penicillin, 100 μg/mL streptomycin (Sigma), and 2 mmol/L glutamine (Bio Whittaker Europe). The cells where grown and incubated in 75 cm^2 flasks (Nunc) at 37°C in a humidified atmosphere containing 5% CO_2.

PDT Treatment and Sample Preparation to SDS-PAGE

NuTu-19 cells were seeded out in 63 cm^2 wells (400,000 per well; Nunc) 6 h before an 18-h incubation with 0.2 μg/mL $TPPS_{2a}$. In some experiments, the cells were washed once with drug-free medium and immediately exposed to light from LumiSource (PCI Biotech) consisting of four light tubes, which deliver blue light with a peak at 435 nm and a fluence rate of 13.5 mW/cm^2. In other experiments, cells were washed twice after photosensitizer incubation and chased for 4 h in drug-free medium before light exposure from LumiSource. WiDr cells were seeded out (600,000 per well) 24 h before 0.4 μg/mL $TPPS_{2a}$ incubation. The cells were washed twice with drug-free medium and incubated for 4 h with new drug-free medium before they were exposed to light from LumiSource. After the PDT treatment, cells were incubated at 37°C until the time of harvest. In the experiments where phosphatase inhibitors were used, sodium orthovanadate ($NaVO_4$; Sigma) was administrated to a final concentration of 1 mmol/L 2 h before exposure to light or okadaic acid (Sigma) was added to a final concentration of 1 μmol/L 30 min before exposure to light and the inhibitors remained in the medium until the time of harvest. The samples for testing the efficacy of the different MAPK inhibitors were

achieved by incubating the NuTu-19 cells with 50 μmol/L PD98059 (MEK inhibitor), 20 μmol/L SB203580 (p38 inhibitor), or 5 μmol/L SP600125 (JNK inhibitor) 1 h before light exposure. The inhibitors remained in the medium until the time of harvest: 5 min after light exposure for the MEK and p38 inhibitor and 2 h for the JNK inhibitor.

NuTu-19 and WiDr cells were harvested 5 min, 2 h, and 24 h after light exposure, except in the experiments where dose-dependent activation of JNK was studied where the NuTu-19 cells were harvested 1 h after exposure to light. Control samples were collected at the same time as the 2-h sample. Harvesting was done on ice by washing the monolayers once with ice-cold PBS before 100 μL lysis buffer (as recently described; ref. 14) was added. Benzonase (1 μL; Merck) was added to each sample before the samples were aliquoted and frozen at -80°C until use. When cells were stimulated with EGF in addition to PDT, EGF (Sigma) was added directly to the cell medium to a final concentration of 100 ng/mL and incubated for 2 min at room temperature before the wells were placed on ice and harvested. At least three independent sets of samples were prepared for each treatment. Toxicity of the *in vitro* PDT treatment was controlled by the 3-(4,5-dimethylthiazol-2-yl)-2,5-diphenyltetrazolium bromide method as explained before (14). Briefly, the cells were incubated for 1 to 3 h with 0.25 mg/mL 3-(4,5-dimethylthiazol-2-yl)-2,5-diphenyltetrazolium bromide reagent (Sigma) 24 h after light exposure. The medium was then removed and the formazan crystals were dissolved in DMSO. Absorbance from formazan was measured at 570 nm, and viability was calculated relative to untreated cells.

SDS-PAGE, Western Blotting, and Immunostaining of Membranes

All samples prepared for protein signaling studies were subjected to SDS-PAGE, Western blotting, and immunostaining. Equivalent amounts of lysed cells (calculated from the nucleic absorption as earlier described; ref. 14) were subjected to gel electrophoresis on 12% SDS-PAGE and blotted to Hybond-P polyvinylidene difluoride membranes (Amersham Biosciences). Immunodetection was carried out using primary antibodies from Cell Signaling Technology (ERK1/2, phospho-ERK1/2, p38, phospho-p38, phospho-MAPKAPK-2, JNK, phospho-JNK, and phospho-c-Jun) and one antibody from Santa Cruz [MAPK phosphatase-1 (MKP-1)]. Horseradish peroxidase–labeled rabbit (Promega) and mouse (Amersham Biosciences) antibodies were used as secondary antibodies. Enhanced Chemiluminescence Plus Western Blotting Detection System, STORM, and Image Quant (GE Healthcare) were used to detect protein bands and to calculate band intensity. Even loading of proteins was verified by the result that total protein did not change between the samples, even unspecific antibody binding in different samples, and/or by Ponceau staining of the membranes. Ponceau staining was done by incubating the membranes in a solution of 0.1% Ponceau (Sigma) and 5% acetic acid for 5 min. The red color was rinsed off with distilled water until only the proteins were stained.

Statistic Evaluations of the Western Blots

The Software Sigma Plot 10 with integrated Sigma Stat (Systat Software) was used for statistic calculations. The relative values of the band intensities were compared by *t* tests or the nonparametric Mann-Whitney test depending on whether the data fulfilled the criteria for approximate normality. In some experiments, this was achieved by a log transformation of the data. At least three independent data sets were included in each test. A two-sided significance level of $P = 0.05$ was used.

Influence of Activation of ERK, p38, and JNK on Viability after PDT and PCI

NuTu-19 cells (2,500 per well) were seeded out in 96-well plates (Nunc) 6 h before an 18-h incubation period with 0.2 μg/mL $TPPS_{2a}$ (PDT samples) and 5 μg/mL gelonin (Sigma; PCI samples). Cells were then washed three times with drug-free medium and chased 3 h before new medium with 50 μmol/L of the MEK inhibitor PD98059 (Sigma), 20 μmol/L of the p38 inhibitor SB203580 (Calbiochem), or 5 μmol/L of the JNK inhibitor SP600125 (Calbiochem) was added. The cells were incubated with the inhibitors for 1 h before being exposed to light from LumiSource. The inhibitors were kept in the cell medium until 2 h after light exposure when the monolayers were washed with fresh medium and incubated until viability was measured with the 3-(4,5-dimethylthiazol-2-yl)-2,5-diphenyltetrazolium bromide method 48 h after light exposure as explained above. The experiments were reproduced twice. The same procedure was followed for the WiDr cells with both the MEK and the p38 inhibitor, except that the cells were allowed to attach to the wells for 24 h before incubation with 0.4 μg/mL $TPPS_{2a}$ and 5 μg/mL gelonin.

Results

$TPPS_{2a}$ is an efficient photosensitizer for use in PCI and this photosensitizer has been shown to enhance the biological effect of several macromolecular drugs *in vitro* (3). When PCI is done, the photosensitizer first attaches to the plasma membrane before it is endocytosed. One may therefore face scenarios where different amounts of the photosensitizer still are present at the plasma membrane at the time of light exposure (14). The present study includes experimental setups to evaluate the importance of plasma membrane located photosenitizer. This is exerted by including or not a 4-h chase in photosensitizer-free medium after the photosensitizer treatment before exposure to light (14).

The toxicity of the PDT treatment regimes used in the Western blot sample preparation has been reported previously (14). If not otherwise described, the PDT doses used in this study reduced the cell viability by 30% to 50% in both cell lines as measured by the 3-(4,5-dimethylthiazol-2-yl)-2,5-diphenyltetrazolium bromide method 24 h after light exposure.

$TPPS_{2a}$-PDT Activates ERK

$TPPS_{2a}$-PDT had no effect on total ERK in NuTu-19 or WiDr cells irrespective of chasing in drug-free medium and EGF treatment (Fig. 2A and *B*). However, $TPPS_{2a}$-PDT in

chased cells that were not stimulated with EGF induced an immediate activation of ERK that lasted for about 2 h, increasing the phospho-ERK/total ERK ratio by ~8-fold in NuTu-19 and ~6-fold in WiDr 5 min after PDT (Fig. 2A and B; Table 1). When the cells were stimulated with EGF 2 min before harvesting, the PDT-induced activation of ERK was much less pronounced compared with control cells treated with EGF only (Fig. 2A and B; Table 1). In chased WiDr cells, a second ~6-fold increase in the phospho-ERK/ERK ratio was observed 24 h after PDT in non-EGF-stimulated cells but was also less pronounced when the cells were treated with EGF before harvesting (Fig. 2B).

Influence of EGF on ERK Activation in PDT-Treated Cells

The results of the Western blot analyses as presented in Fig. 2A and B are relative values to untreated and EGF only–treated cells and the blots with and without EGF cannot be directly compared. In the same experimental setup, where a direct comparison can be made, EGF was found to increase ERK phosphorylation ~3.5-fold in NuTu-19 cells not subjected to PDT and ~1.5-fold in PDT-treated cells 5 min and 2 h after light exposure (Fig. 2C; Table 1). In WiDr cells, EGF induced a ~2.5-fold activation of ERK in non-PDT-treated cells and ~1.5- and ~4-fold activation 5 min and 2 h after PDT, respectively (Fig. 2C; Table 1). Thus, EGF is able to stimulate ERK activation in both untreated and PDT-treated cells. Although the relative fold increase of ERK activation after EGF stimulation varied with time after light exposure (Fig. 2C), the absolute effect of EGF on ERK phosphorylation seemed to be similar in all time points (Fig. 2C). The concentration of EGF used in these experiments where optimal for ERK activation since a 10-fold increase in EGF had no influence on the level of ERK phosphorylation (Fig. 2D). Interestingly, PDT in combination with 100 ng/mL EGF increased the level of ERK phosphorylation 5 min after light exposure above the level of ERK phosphorylation achievable with EGF alone (Fig. 2D).

Influence of Phosphatases on the ERK Activation Profile

Tong et al. have reported that ERK activation after Photofrin-PDT may be regulated by MKP-1 (15). These authors found that MKP-1 expression was increased shortly after PDT and that this activation correlated with a concomitant dephosphorylation of ERK. It was therefore examined whether the phosphorylation of ERK in $TPPS_{2a}$-PDT-treated NuTu-19 cells was regulated by expression of phosphatases. Figure 3A shows that MKP-1 expression increases 3- to 4-fold 2 h after $TPPS_{2a}$-PDT in both EGF-stimulated and unstimulated NuTu-19 cells. The increased

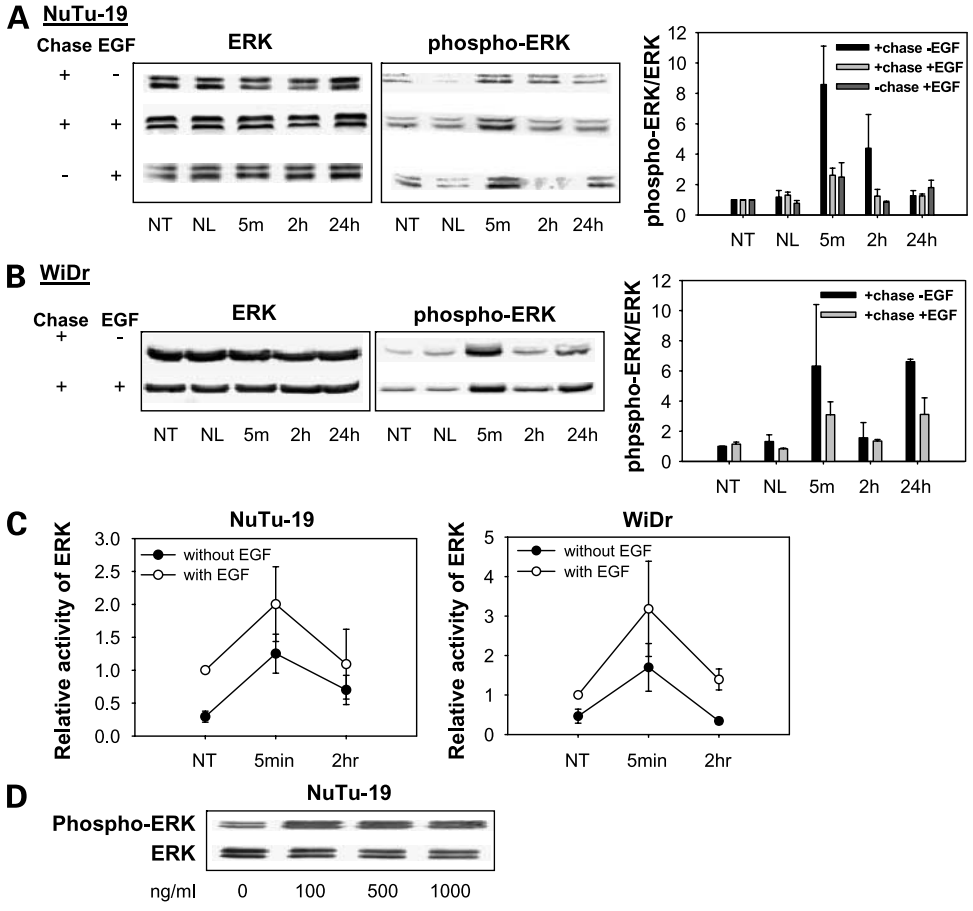

Figure 2. ERK expression and phosphorylation at different time points after $TPPS_{2a}$-PDT with and without 4-h chase of the photosensitizers before light exposure and stimulation with EGF 2 min before harvesting of NuTu-19 cells (**A**) and WiDr cells (**B**). Quantification of phospho-ERK was normalized to total ERK and presented as the amount relative to that in the non-PDT-treated control (*NT*). Cells and tumors treated with photosensitizer without light (*NL*) were also included. Mean of two or three independent experiments; *bars,* SE. *P* values are presented in Table 1. **C,** level of phospho-ERK/total ERK after PDT in NuTu-19 and WiDr cells with and without EGF stimulation 2 min before harvesting of the cells when all samples were loaded on the same Western blot. Values are relative to cells only stimulated with EGF. Mean of five or three independent experiments for NuTu-19 and WiDr, respectively; *bars,* SE. *P* values are presented in Table 1. **D,** phospho-ERK and total ERK in NuTu-19 cells 5 min after 2-min incubation with increasing concentrations of EGF.

Table 1. Effects of EGF and PDT in NuTu-19 and WiDr cells on the phosphorylation state of the ERK, p38, and MKP-1 proteins

Figure	Protein	X	Y	Effect	P (X - Y)	Test
Fig. 2A	Phospho-ERK/ERK	NT + chase - EGF	5 min + chase - EGF	Increase	0.008	MW
Fig. 2A	Phospho-ERK/ERK	NT + chase - EGF	2 h + chase - EGF	Increase	NS	MW
Fig. 2A	Phospho-ERK/ERK	NT + chase + EGF	5 min + chase + EGF	Increase	NS	MW
Fig. 2A	Phospho-ERK/ERK	NT - chase + EGF	5 min - chase + EGF	Increase	NS	MW
Fig. 2A	Phospho-ERK/ERK	5 min + chase - EGF	5 min + chase + EGF	Decrease	0.017	MW
Fig. 2A	Phospho-ERK/ERK	2 h + chase - EGF	2 h + chase + EGF	Decrease	NS	MW
Fig. 2A	Phospho-ERK/ERK	5 min + chase - EGF	5 min - chase + EGF	Decrease	NS	MW
Fig. 2A	Phospho-ERK/ERK	2 h + chase - EGF	2 h - chase + EGF	Decrease	NS	MW
Fig. 2C	Phospho-ERK NuTu-19	NT + EGF/NT - EGF	5 min + EGF/5 min - EGF	Decrease	0.006	*t* test*
Fig. 2C	Phospho-ERK NuTu-19	NT + EGF/NT - EGF	2 h + EGF/2 h - EGF	Decrease	0.003	*t* test*
Fig. 2C	Phospho-ERK WiDr	5 min + EGF/5 min - EGF	2 h + EGF/2 h - EGF	Increase	0.003	*t* test*
Fig. 3A	MKP-1	NT + chase - EGF	2 h + chase - EGF	Increase	0.008	MW
Fig. 3A	MKP-1	NT + chase + EGF	2 h + chase + EGF	Increase	0.002	MW
Fig. 3A	MKP-1	2 h + chase - EGF	2 h + chase + EGF	Increase	NS	MW
Fig. 4A	Phospho-p38/p38	NT, all treatments	5 min, all treatments	Increase	<0.001	MW
Fig. 4A	Phospho-p38/p38	NT, all treatments	2 h, all treatments	Increase	NS	MW
Fig. 4A	Phospho-p38/p38	NT, all treatments	24 h, all treatments	Increase	NS	MW
Fig. 4A	Phospho-p38/p38	NT, all treatments	NL, all treatments	Increase	NS	MW
Fig. 4B	Phospho-p38/p38	NT + NL, all treatments	5 min, all treatments	Increase	0.006	MW
Fig. 4B	Phospho-p38/p38	NT + NL, all treatments	2 h, all treatments	Increase	0.006	MW
Fig. 4B	Phospho-p38/p38	NT + NL, all treatments	24 h, all treatments	Increase	0.006	MW

NOTE: Pairwise comparison and significance levels (*P*) of differences in the time- and treatment-dependent relative band intensity in the groups referred to in Figs. 2A–4. NT are samples not subjected to photosensitizers or light. NL are samples treated with photosensitizers without light. The different time points are time after light exposure. NS, nonsignificant; MW, Mann-Whitney test.
*Log transformation of data.

expression of MKP-1 observed 2 h after PDT may cause the attenuation of ERK phosphorylation observed at 2 h compared with 5 min after PDT (Fig. 2A). NuTu-19 cells were therefore treated with $NaVO_4$, which inhibits tyrosine phosphatases such as MKP-1 (16, 17), to evaluate the importance of phosphatase activation on the ERK activation profile. $NaVO_4$ was found to increase the level of phospho-ERK in non-PDT-treated NuTu-19 cells (Fig. 3B). $NaVO_4$ was also shown to inhibit the increase of MKP-1 expression 2 h after PDT but had no effect on the ERK activation profile after the photodynamic treatment (Fig. 2B and C). Similar results were obtained by treatment with okadaic acid, which inhibits threonine and serine phosphatases (data not shown). The importance of ERK phosphatases on the ERK activation profile in NuTu-19 cells after $TPPS_{2a}$-PDT is therefore questionable.

$TPPS_{2a}$-PDT Activates p38

Total p38 expression was not affected by $TPPS_{2a}$-PDT in either cell line. In the NuTu-19 cell line, a transient 3- to 4-fold increase in phospho-p38/p38 was observed 5 min after PDT and the level of activated p38 was reduced to the level of untreated cells 24 h later (Fig. 4A). A similar activation of p38 in NuTu-19 cells was observed independently of the amount of photosensitizers retained on the plasma membrane at the time of light exposure and stimulation with EGF (Fig. 4A). PDT on WiDr cells also resulted in ~4-fold increase in phospho-p38/p38 5 min after light exposure independent of the different treatment regimes (Fig. 4B). The activation of p38 was, however, more sustained in WiDr cells than in NuTu-19 cells and was in the former still observed 24 h after PDT. Photosensitizer without light exposure did not influence on p38 phosphorylation in WiDr cells (Western blot not shown). Photosensitizer or EGF alone did not alter the level of p38 phosphorylation in either cell line (results not shown).

$TPPS_{2a}$-PDT Activates JNK in NuTu-19 Cells

No change in total JNK was observed after PDT in the two cell lines (Fig. 5A) JNK was not activated by $TPPS_{2a}$-PDT in WiDr cells, whereas a detectable activation of JNK was observed 2 h after $TPPS_{2a}$-PDT in four of eight experiments in NuTu-19 cells (results not shown). In contrast to ERK and p38, no activation of JNK was observed 5 min after light exposure in these experiments, but phosphorylation of JNK was pronounced 1 to 3 h after PDT and was returned to the basal level at 24 h (results not shown). Studies with increasing light doses in NuTu-19 cells showed that the activation of JNK was dose dependent when measured at 1 h after light exposure and JNK was not strongly activated at doses killing <50% of the cells (Fig. 5B). The reason for the variation in phospho-JNK detection after light exposure reported above may therefore be due to the treatment dose killing between 30% and 50% of the cells and thereby causing phosphorylation of JNK on the detection limit of our procedure.

p38 Phosphorylation Serves as a Death Signal, Whereas JNK Phosphorylation Is a Rescuing Signal following $TPPS_{2a}$-PDT

The immediate activation of ERK after PDT observed in this study was inhibited by using an inhibitor of MEK,

PD98059, which is a protein directly upstream of ERK. PD98059 was added 1 h before and removed 2 h after light exposure, an incubation procedure concurrent with the ERK activation pattern after PDT. The ERK activation 5 min after PDT was found to be blocked in the NuTu-19 cells by the treatment with PD98059. The inhibition of MEK did not alter relative viability in PDT, PCI, or untreated NuTu-19 nor WiDr cells (Fig. 6A; data not shown). In WiDr cells, the activation of ERK showed a second boost 24 h after light exposure (Fig. 2B). However, a prolonged incubation of the WiDr cells with PD98059 resulted in significant reduction in cell viability (by 70% after 24 h of incubation) and was therefore not done.

The p38 inhibitor SB203580, however, attenuated both PDT- and PCI-induced toxicity in NuTu-19 cells when added 1 h before and removed 2 h after light exposure (Fig. 6B). At a light dose where PDT alone reduced the viability to 5% of that in untreated cells, SB203580 increased the viability 10-fold to 50% viability, and similar results were observed for the PCI samples. The resistance of SB203580-treated NuTu-19 cells to PDT and PCI indicate that the p38 phosphorylation observed shortly after PDT is an immediate death signal. The p38 inhibitor alone did not affect the viability of the cells. The ability of SB203580 to inhibit PDT-induced activation of p38 in NuTu-19 cells was controlled on Western blot, showing that SB203580 abolished the activation of MAPKAPK-2, a protein downstream of p38. SB203580, when added 1 h before and removed 2 h after light exposure, also showed a tendency to inhibit PDT-induced toxicity in WiDr cells although to a lesser extent than in NuTu-19 cells and only significantly in one of three experiments (results not shown). The p38 activation signal was more sustained in WiDr cells compared with NuTu-19 cells (Fig. 4B), and experiments with the p38 inhibitor present for 24 and 48 h after light exposure were therefore done. However, this treatment caused a reduction in cell viability from the inhibitors alone by >60% and was not done.

The toxic effect of PDT was, in contrast to the p38 inhibitor, increased in the NuTu-19 cell line in the presence of the JNK inhibitor SP600125 at doses where PDT reduced the viability by ≥50% compared with untreated cells (Fig. 6C). At a light dose where PDT alone reduced the viability by 50%, addition of the JNK inhibitor reduced the viability further to 20% of that in untreated cells. The increase in PDT-mediated toxicity by the JNK inhibitor

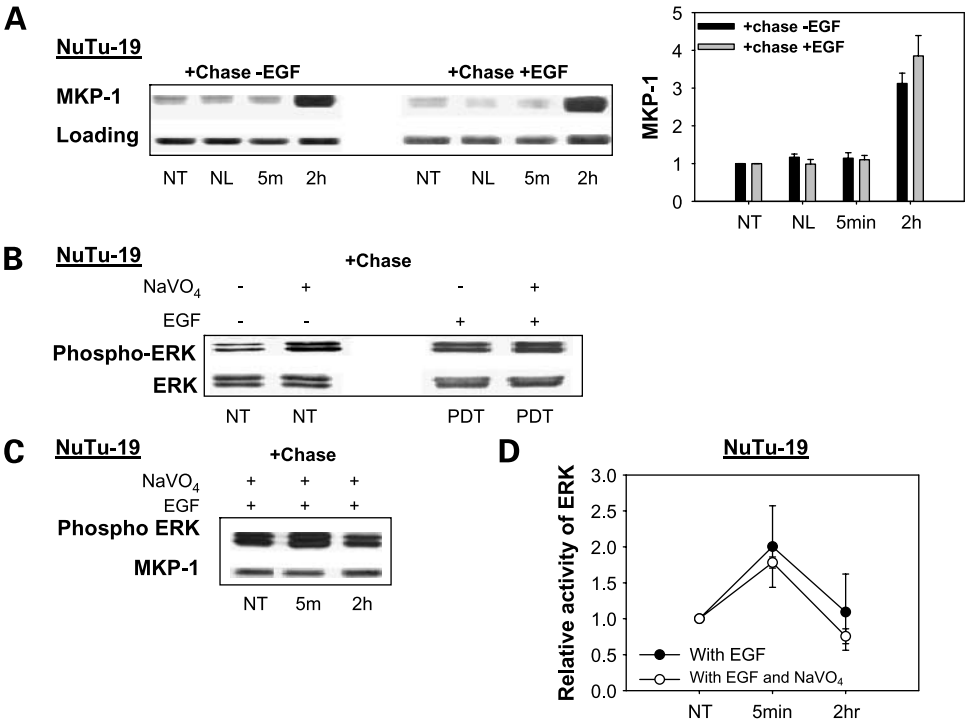

Figure 3. **A,** MKP-1 expression in NuTu-19 cells at different time points after $TPPS_{2a}$-PDT with 4-h chase of the photosensitizers before light exposure with and without stimulation with EGF 2 min before harvesting. The amount of MKP-1 was normalized to that in non-PDT-treated cells. Mean of three independent experiments; *bars,* SE. *P* values are presented in Table 1. **B,** effect of $NaVO_4$ on ERK phosphorylation in untreated and PDT-treated cells after 4-h chase of the photosensitizers before light exposure. The cells were harvested 5 min after light exposure and stimulated with EGF 2 min before harvesting when indicated. **C,** effect of $NaVO_4$ on PDT-induced ERK phosphorylation and MKP-1 expression after 4-h chase of the photosensitizers before light exposure and stimulation with EGF 2 min before harvesting. **D,** level of phospho-ERK/total ERK after PDT with 4-h chase of the photosensitizers before light exposure and 2-min stimulation with EGF before harvesting of NuTu-19 cells. *Open circles,* treated with $NaVO_4$ from 2 h before light exposure until harvesting; *closed circle,* same data as the *open circles* in Fig. 4B. Values are relative to non-PDT-treated cells. Mean of five and three independent experiments for samples with EGF and EGF + $NaVO_4$, respectively; *bars,* SE.

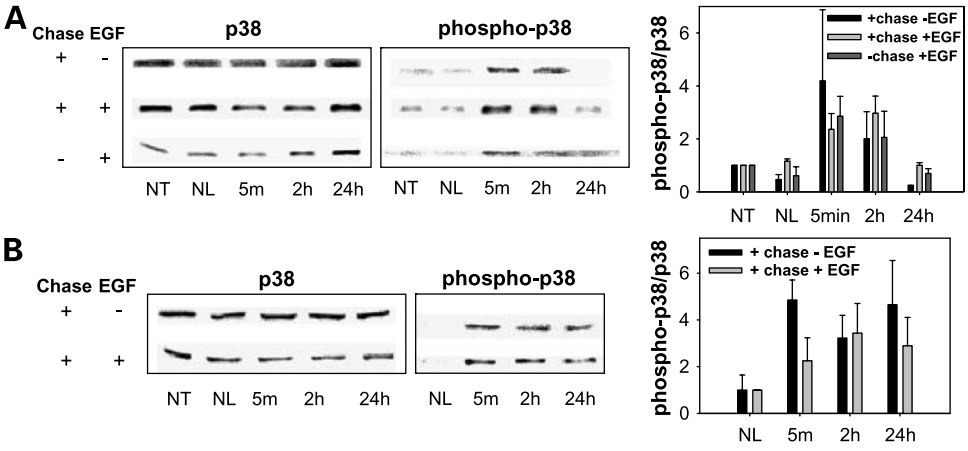

Figure 4. p38 expression and phosphorylation at different time points after TPPS$_{2a}$-PDT with and without 4-h chase of the photosensitizers before light exposure and stimulation with EGF 2 min before harvesting of NuTu-19 cells (**A**) and WiDr cells (**B**). Quantification of phospho-p38 was normalized to total p38 and presented as the amount relative to that in the non-PDT-treated control or cells treated with photosensitizers without light. Mean of two or three independent experiments; *bars,* SE. *P* values are presented in Table 1.

indicates that the JNK activation (Fig. 5) serves as a rescuing and survival signal after TPPS$_{2a}$-PDT. SP600125 alone did not alter viability of the NuTu-19 cells. The ability of the JNK inhibitor to reduce JNK activation was controlled on Western blot, showing that SP600125 attenuated PDT induced activation of c-Jun, a protein downstream of JNK (Fig. 6C). SP600125 seemed to have little influence on cell viability after PCI of gelonin with doses killing up to 90% of the cells. However, at higher PCI doses, SP600125 enhanced the cytotoxic effect (data not shown).

Discussion

Intracellular signaling mechanisms regulating both death and survival have been studied after PDT, and signal transduction is shown to be dependent on the photosensitizer, the cell line and the PDT dose used (11). This is, however, the first report on MAPK protein signaling after PDT with a photosensitizer relevant for PCI. ERK, p38, and JNK are involved in the regulation of growth, differentiation, survival, and death of cells, and the results presented here show that TPPS$_{2a}$-PDT interact with these proteins as a part of its mechanism of action.

The present study shows that TPPS$_{2a}$-PDT activates ERK and this is in contrast to what has been shown after aminolevulinic acid-PDT (18), Photofrin-PDT with 1 h incubation of the photosensitizers (18), and Hypericin-PDT (19), where a reduction in phospho-ERK is reported. The present results are, however, in agreement with Tong et al. who reported that PDT after 18-h incubation with Photofrin activates ERK (15). The similarity between the present results and the report by Tong et al. may be due to concurrent localization of TPPS$_{2a}$ and Photofrin. Photofrin is a mixture of several porphyrins, which localize to different membrane structures of the cells dependent on the experimental setup and the cell line. In general, Photofrin-PDT targets mainly the mitochondria; however, there are indications that Photofrin may be partly or even mainly localized in endocytic vesicles in some cell lines (20, 21). Photofrin-PDT has also been shown to target endoplasmic reticulum (22), and as TPPS$_{2a}$ relocalizes to endoplasmic reticulum after light exposure (23), it has been argued that photochemical targeting of endoplasmic reticulum contributes to the cytotoxic effects of TPPS$_{2a}$-PDT (24). Moreover, oxidative stress is well known to activate ERK by many mechanisms: activation of EGFR, activation of Src kinases,

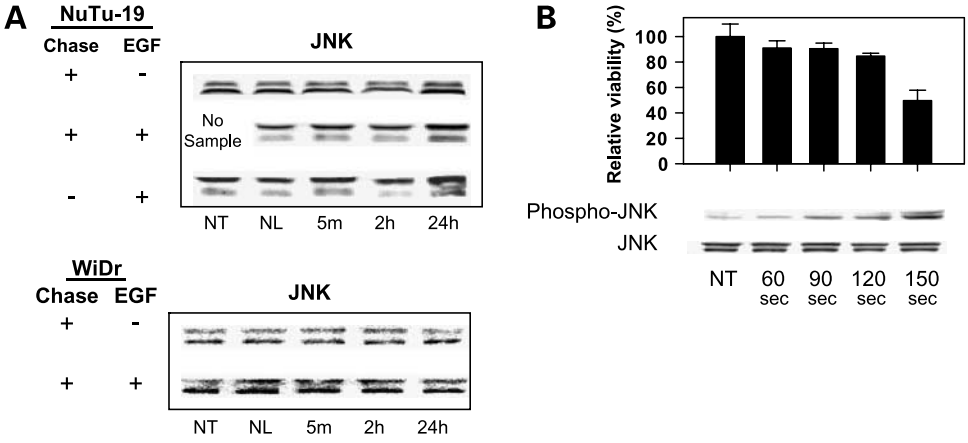

Figure 5. JNK expression at different time points after TPPS$_{2a}$-PDT with and without 4-h chase of the photosensitizers before light exposure and stimulation with EGF 2 min before harvesting of NuTu-19 cells and WiDr cells (**A**). **B,** light dose-dependent activation of JNK in NuTu-19 cells measured 1 h after PDT. Viability of the cells after the treatments as measured by the 3-(4,5-dimethylthiazol-2-yl)-2,5-diphenyltetrazolium bromide method. *Bars,* SE of three parallels.

direct activation of Ras, increased Ca^{2+} influx, and inhibition of phosphatase activity (13). We have reported recently that $TPPS_{2a}$-PDT attenuates EGF-induced activation of EGFR (14), and it is therefore not likely that the ERK phosphorylation observed after $TPPS_{2a}$-PDT in this study is mediated through EGFR. The activation of ERK could be caused by a photochemical damage of phosphatases such as MKP-1. As shown in Fig. 3B, $NaVO_4$ and PDT seem to activate ERK to a similar extent, but the Western blot in Fig. 3A shows no attenuation of the phosphatase 5 min after PDT (Fig. 3A). However, because the active site of MKP-1 is located near the NH_2 terminal of the protein, whereas the MKP-1 antibody recognizes the COOH terminal, it cannot be excluded that photochemical damage in the active site of MKP-1 can take place without detecting any change in the cellular MKP-1 level.

Rose Bengal-PDT, aminolevulinic acid-PDT, and Photofrin-PDT have been reported to cause a loss of responsiveness to growth factors by photochemical targeting of EGFR (18, 19, 25), and as $TPPS_{2a}$-PDT is shown to attenuate EGFR activation after EGF stimulation in the NuTu-19 cell line, it was considered most likely that the EGFR downstream signaling in NuTu-19 cells would be affected by $TPPS_{2a}$-PDT (14). This study shows, however, that although EGF-mediated EGFR activation is attenuated, the absolute phosphorylation of ERK by EGF is not reduced after PDT (Fig. 2C). This may indicate that a rate-limiting step in EGF-mediated ERK phosphorylation is located downstream of EGFR. It is also possible that a negative feedback

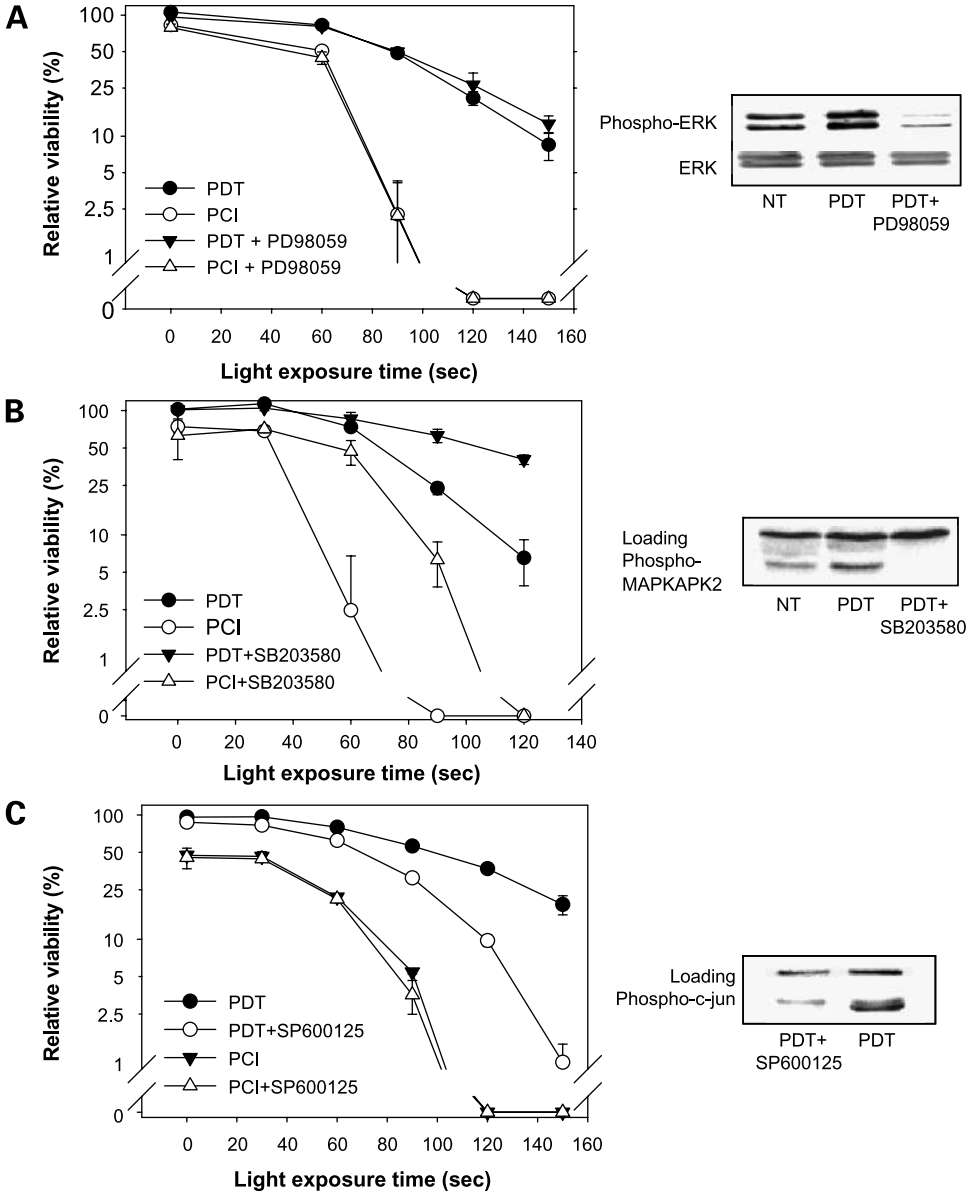

Figure 6. PDT and PCI of gelonin in combination with the MEK inhibitor PD98059 (**A**), the p38 inhibitor SB203580 (**B**), and the JNK inhibitor SP600125 with increasing light doses in NuTu-19 cells. The cells were incubated for 18 h with photosensitizers and gelonin followed by a 4-h chase period before exposure to light. Incubation of the inhibitors was done the last hour of the chasing period until 2 h after light exposure. Cell viability was measured 48 h after light exposure. Mean relative to untreated control cells of triplicates for each light dose; *bars,* SD. Western blots show the effect of the three inhibitors on PDT-mediated activation of ERK and p38 30 min after light exposure and JNK 2 h after light exposure.

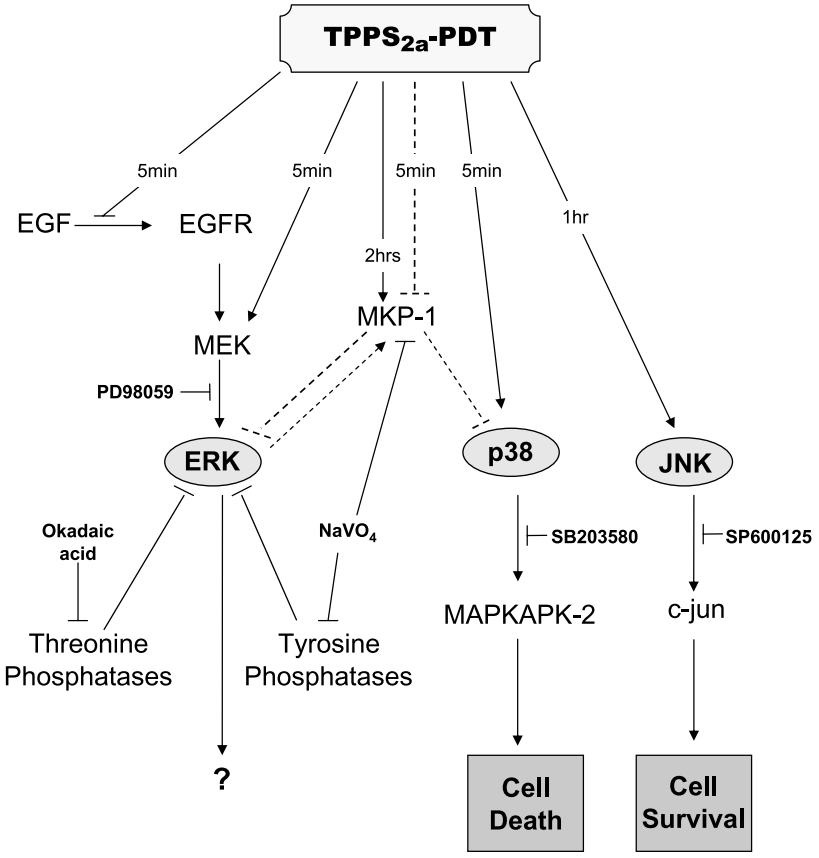

Figure 7. Summary of the effects on signal transduction after $TPPS_{2a}$-PDT reported in the present study. *Arrows,* activation; ⊤, inhibition; *fully drawn arrowed lines,* activations based on results from the present article and also in recently published work (14); *dotted lines,* uncertain but suspected signaling based on the present findings. JNK activation is cell line dependent.

mechanism inhibits ERK activation by EGF in non-PDT-treated cells but not in PDT-treated cells due to reduced activation signal. It has been reported that the protein Raf-1 can function as a negative regulator as well as a stimulator in the EGFR/Ras/Raf/MEK/ERK cascade depending on the sites of phosphorylation, and inhibitory phosphorylation sites on Raf are activated by ERK, indicating a negative feedback mechanism in the cascade (26). It was found that EGF-induced ERK activation is maximal after treatment with 100 ng/mL EGF and that a further increase in the EGF dose does not change the level of ERK phosphorylation. Surprisingly, it was found that EGF stimulation of photochemically treated cells increased the phospho-ERK level above the maximum level inducible by EGF. These results also indicate a rate-limiting step in the EGFR-ERK signaling cascade downstream of EGF and shows that PDT stimulates ERK activation at a level downstream of this rate-limiting step.

The activation of ERK observed 5 min after PDT was transient in both cell lines and declined after 2 h. An increased expression of MKP-1 observed 2 h after PDT seemed to parallel the kinetics of inactivation of ERK as reported by Tong et al., who argued that MKP-1 was a negative regulator of ERK after Photofrin-PDT (15). The present results are, however, not in accordance with Tong et al. because the immediate activation of ERK in NuTu-19 cells declined to a similar extent irrespective of inhibition of MKP-1 expression. Tong et al. also showed that the immediate activation of ERK after Photofrin-PDT correlates with PDT resistance and that the activation of ERK serves as a rescue signal after Photofrin-PDT. This is also in contrast to the present study, where no increased cell death was observed when PDT and PCI were done in the presents of the MEK inhibitor PD98059. Reactive oxygen species–induced activation of ERK has been shown to stimulate both death and survival dependent on the experimental treatment regime (13). We find it interesting that the strong ERK activation observed here seems to have no direct influence on cell survival, and the role of this immediate signal must be further investigated.

The p38 MAPK serves as a part of a signaling cascade controlling cellular responsiveness to cytokines and stress stimuli. The protein cascade eventually activates multiple transcription factors regulating cell survival and death like p53, Max/Myc, Stat1, and ELK-1 (13). PDT with different photosensitizers has been shown to activate p38. The function of this activation seems, however, to depend on both the photosensitizers and the cell line used. Zhuang et al. have reported that p38 phosphorylation observed shortly after Rose Bengal-PDT activates caspase-3 and participates in an apoptotic process (27) and p38 activation has also been linked to Pc4-PDT-mediated apoptosis by the group of Oleinick (28). On the other hand, p38 phosphorylation has been shown to protect cells from

Hypericin-PDT (19), in contrast to Photofrin-PDT where p38 activation seems to have no influence on the treatment outcome (29). Activation of p38 by PDT has also been associated with induction of VEGF following both hypericin-mediated and benzoporphyrin derivative monoacid ring A–mediated PDT (30, 31). The present report indicates that activation of p38 is an immediate death signal after $TPPS_{2a}$-PDT. Oxidative stress can activate p38 by different mechanisms; direct or indirect activation of apoptosis signal-regulating kinase 1 or MKK1-4, activation of growth factors, and activation of members of the tumor necrosis factor family of receptors (13). Little is known about the molecular mechanism behind PDT-induced p38 activation. Hendrickx et al. have shown that phospholipase A2 contributes to the p38 activation following Hypericin-PDT, but because p38 activation is a survival signal after Hypericin-PDT, whereas it serves as a death signal in $TPPS_{2a}$-PDT, we believe the activation after $TPPS_{2a}$-PDT is caused by other mechanisms. As shown for phospho-ERK in Fig. 3B, we have also observed that p38 phosphorylates on administration of $NaVO_4$, and it is possible that the PDT-mediated p38 activation reported here is caused by photochemical damage of phosphatases as proposed for the ERK activation above. Further studies must, however, be done to conclude on the mechanisms controlling $TPPS_{2a}$-PDT-induced activation of p38.

JNK is known to be activated by a variety of environmental stresses like UV, γ-radiation, and cytokines (13). The JNK protein cascade can activate several transcription factors like c-Jun, ATF-2, Elk-1, p53, and STAT3, and as for p38, stress-activated JNK can induce both rescuing and killing signaling. PDT has been shown to activate JNK with different photosensitizers (11, 18, 19) and we also show here that $TPPS_{2a}$-PDT induces a dose-dependent activation of JNK in NuTu-19 cells. Assefa et al. have reported that activation of JNK protects HeLa cells from Hypericin-PDT (19), whereas Hsieh et al. have shown that activation of JNK have little effect on Photofrin-PDT triggered cell death (32). Because the activation of JNK reported here occurs ~1 h later than the immediate p38 and ERK activation, JNK is probably activated by different mechanisms than both p38 and ERK. As the activation of JNK seems to rescue cells from $TPPS_{2a}$-mediated PDT, the mechanisms behind the activation should be further explored.

In conclusion, $TPPS_{2a}$-PDT induces MAPK signaling as presented in Fig. 7. The PDT-induced effects on ERK, p38, and JNK signaling reported here are not dependent on the amount of the photosensitizers localized on the plasma membrane at the time of light exposure. The present report shows that the MAPK signaling after $TPPS_{2a}$-PDT is not dependent on EGFR activation and will therefore probably not be affected by PCI of EGFR targeting drugs using EGF or cetuximab as targeting ligands. Mapping the intracellular signal transduction after PDT is important to understand the mechanism of action that induce cell death after PDT and PCI and can probably be used to predict drugs suitable for PCI. PCI can be considered as a multimodality therapy between PDT and the drug of interest. Combination therapy strategies are becoming increasingly relevant in the treatment of cancer, and enhanced therapeutic effects have been shown by combining PDT with other anticancer agents (33–35). The present report adds important information for PCI as well as molecular response-based combination therapy strategies with PDT.

Disclosure of Potential Conflicts of Interest

No potential conflicts of interest were disclosed.

Acknowledgments

We thank Marie-Therese Roppestad Strand for valuable laboratory assistance.

References

1. Berg K, Selbo PK, Prasmickaite L, et al. Photochemical internalization: a novel technology for delivery of macromolecules into cytosol. Cancer Res 1999;59:1180 – 3.

2. Hogset A, Prasmickaite L, Selbo PK, et al. Photochemical internalisation in drug and gene delivery. Adv Drug Deliv Rev 2004;56:95 – 115.

3. Dietze A, Selbo PK, Prasmickaite L, et al. Photochemical internalization (PCI): a new modality for light activation of endocytosed therapeuticals. J Environ Pathol Toxicol Oncol 2006;25:521 – 36.

4. Oliveira S, Fretz MM, Hogset A, Storm G, Schiffelers RM. Photochemical internalization enhances silencing of epidermal growth factor receptor through improved endosomal escape of siRNA. Biochim Biophys Acta 2007;1768:1211 – 7.

5. Selbo PK, Sivam G, Fodstad O, Sandvig K, Berg K. *In vivo* documentation of photochemical internalization, a novel approach to site specific cancer therapy. Int J Cancer 2001;92:761 – 6.

6. Ndoye A, Dolivet G, Hogset A, et al. Eradication of p53-mutated head and neck squamous cell carcinoma xenografts using nonviral p53 gene therapy and photochemical internalization. Mol Ther 2006;13:1156 – 62.

7. Nishiyama N, Iriyama A, Jang WD, et al. Light-induced gene transfer from packaged DNA enveloped in a dendrimeric photosensitizer. Nat Mater 2005;4:934 – 41.

8. Berg K, Dietze A, Kaalhus O, Hogset A. Site-specific drug delivery by photochemical internalization enhances the antitumor effect of bleomycin. Clin Cancer Res 2005;11:8476 – 85.

9. Weyergang A, Selbo PK, Berg K. Photochemically stimulated drug delivery increases the cytotoxicity and specificity of EGF-saporin. J Control Release 2006;111:165 – 73.

10. Yip WL, Weyergang A, Berg K, Tonnesen HH, Selbo PK. Targeted delivery and enhanced cytotoxicity of cetuximab-saporin by photochemical internalization in EGFR-positive cancer cells. Mol Pharmacol 2007;4:241 – 51.

11. Almeida RD, Manadas BJ, Carvalho AP, Duarte CB. Intracellular signaling mechanisms in photodynamic therapy. Biochim Biophys Acta 2004;1704:59 – 86.

12. Moor AC. Signaling pathways in cell death and survival after photodynamic therapy. J Photochem Photobiol B 2000;57:1 – 13.

13. McCubrey JA, Lahair MM, Franklin RA. Reactive oxygen species-induced activation of the MAP kinase signaling pathways. Antioxid Redox Signal 2006;8:1775 – 89.

14. Weyergang A, Selbo PK, Berg K. Y1068 phosphorylation is the most sensitive target of disulfonated tetraphenylporphyrin-based photodynamic therapy on epidermal growth factor receptor. Biochem Pharmacol 2007;74:226 – 35.

15. Tong Z, Singh G, Rainbow AJ. Sustained activation of the extracellular signal-regulated kinase pathway protects cells from Photofrin-mediated photodynamic therapy. Cancer Res 2002;62:5528 – 35.

16. Hulley PA, Conradie MM, Langeveldt CR, Hough FS. Glucocorticoid-induced osteoporosis in the rat is prevented by the tyrosine phosphatase inhibitor, sodium orthovanadate. Bone 2002;31:220 – 9.

17. Kassel O, Sancono A, Kratzschmar J, Kreft B, Stassen M, Cato AC.

Glucocorticoids inhibit MAP kinase via increased expression and decreased degradation of MKP-1. EMBO J 2001;20:7108 – 16.

18. Wong TW, Tracy E, Oseroff AR, Baumann H. Photodynamic therapy mediates immediate loss of cellular responsiveness to cytokines and growth factors. Cancer Res 2003;63:3812 – 8.

19. Assefa Z, Vantieghem A, Declercq W, et al. The activation of the c-Jun N-terminal kinase and p38 mitogen-activated protein kinase signaling pathways protects HeLa cells from apoptosis following photodynamic therapy with hypericin. J Biol Chem 1999;274:8788 – 96.

20. Berg K, Maziere JC, Geze M, Santus R. Verapamil enhances the uptake and the photocytotoxic effect of PII, but not that of tetra(4-sulfonatophenyl)porphine. Biochim Biophys Acta 1998;1370:317 – 24.

21. Prasmickaite L, Hogset A, Berg K. Evaluation of different photosensitizers for use in photochemical gene transfection. Photochem Photobiol 2001;73:388 – 95.

22. Candide C, Maziere JC, Santus R, et al. Photosensitization of Wi26-4 transformed human fibroblasts by low density lipoprotein loaded with the anticancer porphyrin mixture Photofrin II: evidence for endoplasmic reticulum alteration. Cancer Lett 1989;44:157 – 61.

23. Rodal GH, Rodal SK, Moan J, Berg K. Liposome-bound Zn (II)-phthalocyanine. Mechanisms for cellular uptake and photosensitization. J Photochem Photobiol B 1998;45:150 – 9.

24. Berg K, Madslien K, Bommer JC, Oftebro R, Winkelman JW, Moan J. Light induced relocalization of sulfonated *meso*-tetraphenylporphines in NHIK 3025 cells and effects of dose fractionation. Photochem Photobiol 1991;53:203 – 10.

25. Schieke SM, von Montfort C, Buchczyk DP, et al. Singlet oxygen-induced attenuation of growth factor signaling: possible role of ceramides. Free Radic Res 2004;38:729 – 37.

26. Dougherty MK, Muller J, Ritt DA, et al. Regulation of Raf-1 by direct feedback phosphorylation. Mol Cell 2005;17:215 – 24.

27. Zhuang S, Demirs JT, Kochevar IE. p38 mitogen-activated protein kinase mediates bid cleavage, mitochondrial dysfunction, and caspase-3 activation during apoptosis induced by singlet oxygen but not by hydrogen peroxide. J Biol Chem 2000;275:25939 – 48.

28. Xue L, He J, Oleinick NL. Promotion of photodynamic therapy-induced apoptosis by stress kinases. Cell Death Differ 1999;6:855 – 64.

29. Tong Z, Singh G, Valerie K, Rainbow AJ. Activation of the stress-activated JNK and p38 MAP kinases in human cells by Photofrin-mediated photodynamic therapy. J Photochem Photobiol B 2003;71:77 – 85.

30. Hendrickx N, Dewaele M, Buytaert E, et al. Targeted inhibition of p38α MAPK suppresses tumor-associated endothelial cell migration in response to hypericin-based photodynamic therapy. Biochem Biophys Res Commun 2005;337:928 – 35.

31. Solban N, Pal SK, Alok SK, Sung CK, Hasan T. Mechanistic investigation and implications of photodynamic therapy induction of vascular endothelial growth factor in prostate cancer. Cancer Res 2006;66:5633 – 40.

32. Hsieh YJ, Wu CC, Chang CJ, Yu JS. Subcellular localization of Photofrin determines the death phenotype of human epidermoid carcinoma A431 cells triggered by photodynamic therapy: when plasma membranes are the main targets. J Cell Physiol 2003;194:363 – 75.

33. Crescenzi E, Chiaviello A, Canti G, Reddi E, Veneziani BM, Palumbo G. Low doses of cisplatin or gemcitabine plus Photofrin/photodynamic therapy: disjointed cell cycle phase-related activity accounts for synergistic outcome in metastatic non-small cell lung cancer cells (H1299). Mol Cancer Ther 2006;5:776 – 85.

34. Kosharskyy B, Solban N, Chang SK, Rizvi I, Chang Y, Hasan T. A mechanism-based combination therapy reduces local tumor growth and metastasis in an orthotopic model of prostate cancer. Cancer Res 2006;66:10953 – 8.

35. Seshadri M, Spernyak JA, Mazurchuk R, et al. Tumor vascular response to photodynamic therapy and the antivascular agent 5,6-dimethylxanthenone-4-acetic acid: implications for combination therapy. Clin Cancer Res 2005;11:4241 – 50.